Limnol. Oceanogr., 55(4), 2010, 1614–1626

doi:10.4319/lo.2010.55.4.1614

Microbial dimethylsulfoniopropionate (DMSP) dynamics along a natural iron gradient in the northeast subarctic Pacific

Sarah-Jeanne Royer,[a,1] Maurice Levasseur,[a,*] Martine Lizotte,[a] Michael Arychuk,[b] Michael G. Scarratt,[c] Chi Shing Wong,[b] Connie Lovejoy,[a] Marie Robert,[b] Keith Johnson,[b] Angelica Peña,[b] Sonia Michaud,[c] and Ronald P. Kiene[d]

[a] Université Laval, Département de biologie (Québec–Océan), Québec, Québec, Canada
[b] Institute of Ocean Sciences, Fisheries and Oceans Canada, Sidney, British Columbia, Canada
[c] Maurice Lamontagne Institute, Fisheries and Oceans Canada, Mont-Joli, Québec, Canada
[d] University of South Alabama, Department of Marine Sciences, Mobile, Alabama

Abstract

We characterized the effect of an inshore–offshore gradient in Fe in the northeast subarctic Pacific on the bacterioplankton and phytoplankton assemblages and on the microbial cycling of particulate and dissolved dimethylsulfoniopropionate ($DMSP_p$ and $DMSP_d$) and dimethylsulfide (DMS). Averaged concentrations of total dissolved Fe (TDFe) decreased linearly with increasing water density along the transect, from 3.4 nmol L^{-1} at the two inshore stations to 1.0 nmol L^{-1} at the offshore stations, as a result of the vertical and lateral mixing between the Fe-rich coastal water and the Fe-poor Alaska Current. The Fe-rich inshore stations were dominated by diatoms and characterized by low $DMSP_p$: chlorophyll *a* (Chl *a*) ratios (ca. 26 nmol μg^{-1}) and bacterial DMS yield (< 4%). In contrast, the Fe-poor offshore stations were dominated by prymnesiophytes and exhibited high $DMSP_p$: Chl *a* ratios (ca. 84 nmol μg^{-1}) and bacterial DMS yield (8%). Chl *a*, $DMSP_p$, and the abundance of total bacteria and three bacterial clades (*Gammaproteobacteria*, *Roseobacter*, and *Betaproteobacteria*) were positively correlated with the TDFe gradient. At the Fe-poor offshore stations, the positive correlation found between TDFe and the $DMSP_p$: Chl *a* ratios suggests that Fe supplied by mixing stimulated DMSP production in the prymnesiophyte-dominated assemblage, a response similar to that generally observed during the first days of most of the large-scale ocean iron fertilizations (OIFs). These results suggest that the stimulation of DMSP production takes place whatever the Fe supply mode: atmospheric dust deposition, as simulated by OIFs, or mixing, as reported in this study.

The productivity of more than 25% of the world's oceans is limited by Fe (de Baar et al. 1999, 2005). These areas, referred to as high-nutrient, low-chlorophyll (HNLC) regions, are found in the Southern Ocean, the Equatorial Pacific, and the north subarctic Pacific. HNLC regions are supplied with Fe via different mechanisms: sporadically via the deposition of eolian dust (an allochthonous source), by mixing, diffusion, and lateral advection (autochthonous sources) (Jickells et al. 2005). The relative contribution of these natural sources of Fe varies in time and space, with eolian deposition dominating in regions adjacent to and downwind of the dust sources during windy periods, and mixing or advection dominating farther away from these sources.

The potential influence of Fe eolian deposition on biogeochemical cycles has been studied in different HNLC regions by artificially fertilizing large areas (ca. 100 km^2; *see* reviews by de Baar et al. 2005; Boyd et al. 2007). Results from these ocean iron fertilizations (OIFs) suggested that Fe could potentially increase both carbon sequestration and dimethylsulfide (DMS) emissions with a cumulative cooling effect on climate (Turner et al. 2004). OIFs are considered valuable simulations of large sporadic eolian Fe dust deposition events, but their relevance to noneolian Fe delivery processes such as mixing has been questioned (Boyd et al. 2007). Ecosystems and biogeochemical cycles may respond differently to short artificial pulses of Fe, as represented by OIFs, compared with continuous slow addition of Fe through natural autochthonous sources. For example, it was recently shown that natural Fe fertilization through mixing above the Kerguelen plateau in the Southern Ocean HNLC region has no stimulating effect on DMS concentrations, in contrast to increases in DMS measured during the OIFs conducted in the same region (Bopp et al. 2008). However, natural Fe supply events are difficult to monitor, and very few studies have examined their effects on ecosystems and biogeochemical cycles.

DMS is the most important biogenic sulfur compound emitted from the ocean into the atmosphere. Oceanic emissions of DMS influence the climate directly through their oxidation into sulfate aerosols by hydroxyl radicals (OH) and indirectly by the effect of sulfate aerosols on cloud condensation nuclei (CCN) formation with further effects on cloud albedo (Charlson et al. 1987; Andreae 1990). As a consequence, DMS emissions could reduce the radiative flux to the Earth's surface (Charlson et al. 1987) with a resulting cooling effect on the climate. The oceanic production of DMS results from a suite of interrelated biotic processes involving most components of the food web, from viruses to zooplankton (review by Simó 2001). DMS is produced by the algal and bacterial cleavage of

* Corresponding author: maurice.levasseur@bio.ulaval.ca

[1] Current address: Institut de Ciències del Mar (CSIC), Barcelona, Catalonia, Spain

dimethylsulfoniopropionate (DMSP), an osmolyte found in different concentrations in a wide variety of phytoplankton groups (Keller et al. 1989). The composition of the plankton assemblage ultimately governs the production rate of DMSP; the release of algal DMSP into the water via exudation, grazing, or viral attack; the bacterial metabolism of DMSP; and its biological transformation into DMS (Hill et al. 1998; Malin et al. 1998). Fe supply can influence several of these processes, either directly through physiological responses or indirectly through changes in biomass, community structure, and dissolved organic matter. The response of the ocean to Fe supply may thus vary widely depending on initial conditions.

The North Pacific is sporadically supplied with Fe during seasonal eastward dust transport from Asia (Moore et al. 2002; Han et al. 2008). These events often coincide with increases in surface biomass and biogenic material flux at depth (Young et al. 1991; Yuan and Zhang 2006), indicating the stimulating effect of Fe on primary production. Past studies have also identified Asian dust as the main source of Fe to the Alaska Gyre (Moore et al. 2002; Moore and Braucher 2007). However, recent studies have shown that vertical mixing and the offshore advection of eddies from the continental margin of the Gulf of Alaska, two autochthonous supply mechanisms, also represent nonnegligible sources of Fe (Johnson et al. 2005; Crawford et al. 2007; Lam and Bishop 2008). In 2002, a large-scale Fe fertilization was conducted around Ocean Station Papa (OSP) (50°N, 145°W; Subarctic Ecosystem Response to Iron Enrichment Study [SERIES]) in order to explore the potential effect of Fe on the ecosystem and biogeochemical fluxes in the northeast (NE) Pacific (Boyd et al. 2004). One of the unexpected results of this experiment was the decrease in DMS concentrations (Levasseur et al. 2006) despite a strong stimulation of the growth of the DMSP producers. This response was attributed to a shift in the bacterial assimilation of DMSP-derived sulfur (DMSP-S) coinciding with a sharp increase in bacterial growth and sulfur demand, resulting in little DMS production (Merzouk et al. 2006). Whether these results can be extrapolated to other modes of Fe supply, such as mixing, still needs to be determined.

The aim of this study was to characterize the effect of a natural inshore–offshore gradient in Fe availability in the NE subarctic Pacific on the distribution of bacterial and phytoplankton assemblages and to determine how these changes in the planktonic ecosystem affect the microbial metabolism of DMSP (particulate and dissolved) and DMS.

Methods

Study area and sampling scheme—The study was conducted in the Fe-rich coastal waters off Vancouver Island (Canada) and in the HNLC waters of the Gulf of Alaska in the NE subarctic Pacific Ocean, a region that has been monitored over the last 50 yr by various research programs run by the Government of Canada; *see* Freeland (2007) for a review of the Line P cruise program.

From 21 May to 19 June 2007, water samples were collected aboard the CCGS *John P. Tully* at 11 stations located along the Line P transect beginning at the southern tip of Vancouver Island (P1) and ending at OSP (P26; Fig. 1). Water samples for nutrients and chlorophyll *a* (Chl *a*) and pigment measurements were collected at 10 m using a General Oceanics (GO) rosette equipped with 10-liter Niskin bottles coupled to a conductivity, temperature, depth (CTD) probe system model SBE 11 plus (Seabird Electronics). For total dissolved Fe (TDFe), bacteria cell counts, DMSP, and DMS measurements, water samples were collected at 10 m using trace metal clean techniques (Johnson et al. 2005) with a 10-liter GO-FLO bottle at the two inshore stations and with 12-liter Niskin-X GO bottles at open ocean stations. GO-FLO and Niskin-X bottles were mounted on a Kevlar line for sampling. Stas. P1 (114 m) and P4 (1320 m) were located on the continental margin and on the continental slope, respectively. The other stations, P8 to P26, were located in the open ocean with a mean water depth of 3630 m.

Nutrients, Chl a*, and* Fe *analyses*—Concentrations of nitrate + nitrite ($NO_3^- + NO_2^-$), silicic acid (H_4SiO_4), and phosphate (PO_4^{3-}) were analyzed fresh at sea using a Technicon AA autoanalyzer II following the methods described in Barwell-Clarke and Whitney (1996). For Chl *a* determination, 330 mL of seawater was filtered through a glass-fiber 25-mm MFS GF-75 filter (nominal rating 0.3 μm) at $<$ 70 mm Hg vacuum, the pigments collected on the filter were extracted with 90% acetone and quantified with a Turner 10 AU fluorometer as described in Strickland and Parsons (1972). Macronutrients and Chl *a* observations presented in this paper are from single measurements, but the precision for these measurements was determined on a regular basis during the Line P cruise program using pooled standard deviations (Sp) of replicate samples drawn from the same Niskin bottle. Sp was less than 1.1% for nitrate, 6.0% for silicate, and 2.6% for phosphate, while for paired Chl *a* samples, Sp was less than 6.9%. For measurements of Fe, water was filtered (0.22 μm) and collected in acid-washed 125-mL low-density polyethylene bottles and then acidified with 1.0 mL of 6 mol L^{-1} ultrapure hydrochloric acid (HCl; 1 : 1 Seastar Baseline) per 125 mL to get a final concentration of 0.05 mol L^{-1} HCl (pH 1.6). The samples were stored for approximately 3 months prior to analysis following the Obata et al. (1993, 1997) analytical method and further amendments of this method described by Johnson et al. (2005). The acidified and filtered dissolved Fe samples were operationally defined as total dissolved Fe (TDFe) according to the analytical iron fraction definition of Johnson et al. (2005). TDFe analysis was conducted in duplicate.

Pigment analysis—Seawater samples of 1250 mL were collected at 5 of the 11 stations (P4, P12, P16, P20, and P26), filtered through glass-fiber 25-mm AMD GF-75 filters at $<$ 70 mm Hg vacuum, and stored frozen in liquid nitrogen until analysis ashore. Pigments were extracted in 95% methanol at -20°C for 24 h in the dark. The extracts were filtered through 25-mm diameter polytetrafluorothylene syringe filters (0.2-μm pore size) to remove cell and filter debris. The filtrate was mixed with water in a 5 : 1

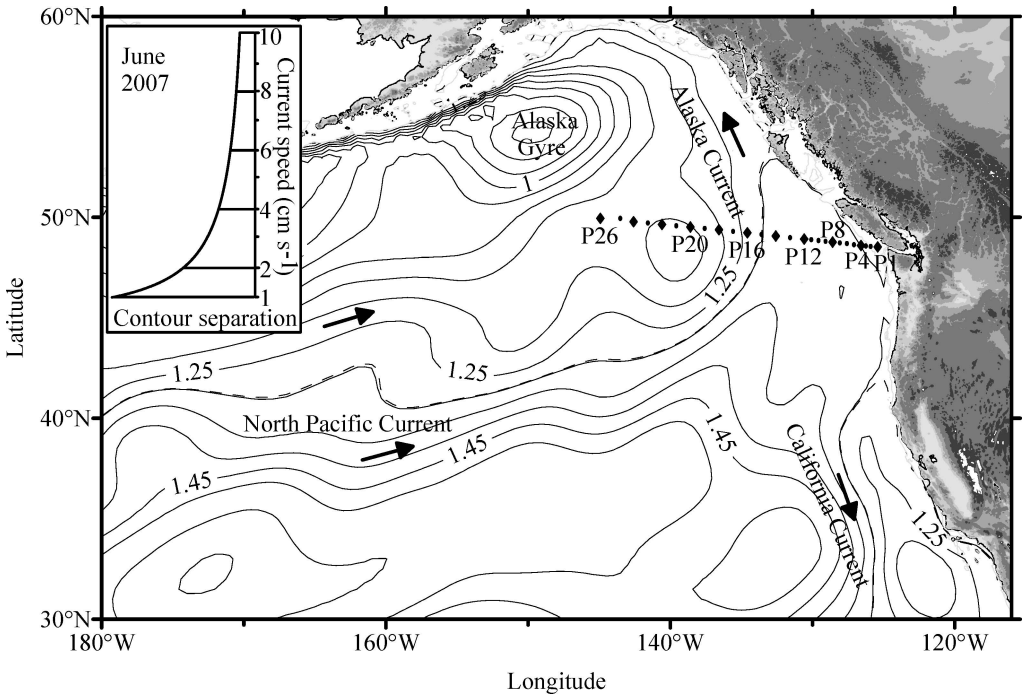

Fig. 1. Study site showing the 11 stations investigated along the Line P transect in the NE subarctic Pacific Ocean between 21 May and 19 June 2007. Sta. P26 is Ocean Station Papa. The circulation map was created by computing the dynamic height at the sea surface relative to 1000 decibars using temperature and salinity observations (n = 350 profiles) obtained from Argo profiling floats. The dashed line represents the dividing streamline separating water that ultimately flows into the Alaska Gyre from that flowing into the California Current. Large diamonds represent sampling stations. Small dots represent other traditional Line P stations not considered in this study.

ratio (volume : volume [v : v]) before injection and analyzed with a Waters Alliance high performance liquid chromatography (HPLC) system equipped with a reverse-phase C8 column using the pyridine-containing mobile phases method (Zapata et al. 2000). Pigment concentrations were quantified using commercially available standards (Danish Hydraulic Institute).

The contribution of each phytoplankton group to Chl *a* biomass was estimated from the concentration of biomarker pigments by using the chemotaxonomy program CHEMTAX (Mackey et al. 1996). Eight algal groups were separated based on their pigment contents: diatoms, prymnesiophytes, pelagophytes, chlorophytes, prasinophytes, cryptophytes, dinoflagellates, and cyanobacteria. The initial pigment ratio matrix loaded into the CHEMTAX program (Table 1A) was obtained by averaging the minimum and maximum values of pigment : Chl *a* ratios given in table 1 of Mackey et al. (1996) and was similar to that used by Suzuki et al. (2002) for samples collected in the subarctic North Pacific. The final pigment : Chl *a* ratios generated by CHEMTAX analysis are shown in Table 1B.

Heterotrophic bacterial abundance and identification—Water samples for bacterioplankton abundance and identification were preserved for 24 h at 4°C with borate-buffered formaldehyde (2% final concentration), filtered onto 0.2-μm pore size, 25-mm diameter polycarbonate membrane filters, and frozen at −20°C until analysis. Cell identification for specific prokaryotic groups was made by fluorescence in situ hybridization (FISH) using horseradish peroxidase (HRP) labeled oligonucleotide probes (www.biomers.net) combined with signal amplification by tyramide labeled with carboxyfluorescein. This catalyzed reporter deposition (CARD) approach has the advantage of providing enhanced fluorescence intensities (Pernthaler et al. 2002) compared with the standard FISH assay. Sections were cut from each filter and hybridized with the HRP probes specific to three major phylogenetic lineages of this latter domain: beta (β; Bet42a), gamma subclasses of the *Proteobacteria* (γ; Gam42a), and the *Roseobacter* clade (Ros536), a clade within *Alphaproteobacteria*.

The CARD-FISH positive cells of the target groups were then determined using epifluorescence microscopy (Pernthaler et al. 2002). Total bacterial abundance was estimated on the same filter sections that had been counterstained with 4′,6′-diamidino-2-phenylindole (DAPI; Porter and Feig 1980). At least 10 fields were counted at ×1000 magnification for each filter, and a minimum of 400 DAPI-stained cells and 100 CARD-FISH positive cells per filter were counted.

DMSP and DMS concentration analysis—DMSP and DMS measurements were conducted in triplicate. DMSP is found in a filterable particulate fraction ($DMSP_p$) and a dissolved fraction ($DMSP_d$). Fractionation of $DMSP_p$ and $DMSP_d$ was determined using the small-volume gravity drip filtration (SVDF) technique (Kiene and Slezak 2006). This technique reduces the release of DMSP from phytoplankton cell breakage. However, the $DMSP_d$ pool remains notoriously difficult to measure, and even the use

Table 1. Biomarker pigment: Chl *a* ratios for eight algal groups: (A) initial ratio matrix, and (B) final ratio matrix obtained by CHEMTAX on the pigment data.

	Chl c_3	Chl c_2	Fucox	19′-but	19′-hex	Peri	Diadinox	Allox	Violax	Prasinox	Chl *b*	Zeax	Chl *a*
(A)													
Diatoms	0	0	0.457	0	0	0	0.239	0	0	0	0	0	1
Prymne	0.238	0	0.583	0.261	0.680	0	0.196	0	0	0	0	0	1
Pelago	0.125	0.127	0.625	0.933	0	0	0.438	0	0	0	0	0	1
Chloro	0	0	0	0	0	0	0	0	0.028	0	0.285	0.059	1
Prasino	0	0	0	0	0	0	0	0	0.114	0.360	0.888	0.142	1
Crypto	0	1.126	0	0	0	0	0	0.136	0	0	0	0	1
Dinofla	0	0.285	0	0	0.192	0.532	0.121	0	0	0	0	0	1
Cyano	0	0	0	0	0	0	0	0	0	0	0	0.334	1
(B)													
Diatoms	0	0	0.749	0	0	0	0.148	0	0	0	0	0	1
Prymne	0.364	0	0.308	0.302	1.139	0	0.454	0	0	0	0	0	1
Pelago	0.125	0.127	0.625	0.919	0	0	0.438	0	0	0	0	0	1
Chloro	0	0	0	0	0	0	0	0	0.028	0	0.285	0.059	1
Prasino	0	0	0	0	0	0	0	0	0.114	0.092	1.164	0.142	1
Crypto	0	0.689	0	0	0	0	0	0.073	0	0	0	0	1
Dinofla	0	0.285	0	0	0.192	0.532	0.121	0	0	0	0	0	1
Cyano	0	0	0	0	0	0	0	0	0	0	0	0.624	1

Abbreviations: Prymne, prymnesiophytes; Pelago, pelagophytes; Chloro, chlorophytes; Prasino, prasinophytes; Crypto, cryptophytes; Dinofla, dinoflagellates; Cyano, cyanobacteria; Chl c_3, chlorophyll c_3; Chl c_2, chlorophyll c_2; Fucox, fucoxanthin; 19′-but, 19′-butanoyloxyfucoxanthin; 19′-hex, 19′-hexanoyloxyfucoxanthin; Peri, peridinin; Diadinox, diadinoxanthin; Allox, alloxanthin; Violax, violaxanthin; Prasinox, prasinoxanthin; Chl *b*, chlorophyll *b*; Zeax, zeaxanthin; Chl *a*, chlorophyll *a*.

of this technique may result in large variability between replicate measurements. Water was gently collected directly from the 10-liter GO-FLO bottle or the 12-liter Niskin-X bottle and poured into a polysulfone magnetic filter tower through a 47-mm Whatman GF/F filter (0.7 μm retention). For $DMSP_d$ determination, between 20 and 50 mL was allowed to fill the filter tower, and 3.5 mL of filtrate was collected into a 15-mL sterile screw-cap centrifuge tube (Falcon) to which 50 μL of 50% H_2SO_4 was added to eliminate the DMS. For total DMSP ($DMSP_t$) determination ($DMSP_t = DMSP_p + DMSP_d$), an unfiltered volume of 3.5 mL was collected and 50 μL of 50% H_2SO_4 was added. DMSP samples were stored at 4°C in the dark for a minimum of 24 h and a maximum of 6 weeks to allow complete acidification of DMS. After this storage period, 25-mL serum bottles were filled with 21 mL of deionized water (milli-Q water), 3 mL of the stored $DMSP_t$ and $DMSP_d$ samples, and 1 mL of 5 mol L^{-1} NaOH. The bottles were then quickly sealed with a butyl stopper and aluminum crimp, leaving no headspace. Subsamples of DMSP, now hydrolyzed into DMS, were drawn from the 25-mL serum vials and sparged in a purge and trap apparatus for 4 min with ultra–high-purity (UHP) helium, and the DMS gas was cryogenically trapped in a Teflon tube maintained in liquid nitrogen. Sulfur gas analysis was then performed using a Varian 3800 gas chromatograph (GC) equipped with a pulsed flame photometric detector and a wall-coated fused silica capillary column (Varian CP7529) (Scarratt et al. 2000). The DMSP concentrations in seawater samples were determined from a standard curve established by injecting different volumes of a 5 ng mL^{-1} DMSP standard prepared in 14-mL serum bottles containing 0.6 mL of KOH 10 mol L^{-1}.

DMS samples were collected using 150-mL serum bottles leaving no headspace and analyzed onboard using a Hewlett-Packard 5880A GC equipped with a Flame Photometric Detector and a Chromasil 330 column (Supelco 1-1496). The samples were initially loaded onto a stripper and purged with UHP nitrogen for 10 min at $\sim$ 100 mL min^{-1}. The extracted DMS was adsorbed onto a Tenax-TA cartridge kept at −80°C. The trap was subsequently desorbed at 100°C onto the GC. Standards were run in the same manner as samples and were prepared in deionized water from a pure stock DMS solution and covered a linear range of 0.5 nmol L^{-1} to 20 nmol L^{-1}. The two DMS methods described in this study generate comparable values (Levasseur et al. 2006).

^{35}Sulfur-DMSP incubations for the determination of microbial DMSP cycling—For the determination of the microbial uptake and metabolism of DMSP, unfiltered seawater was collected at 10 m with ultraclean techniques and transferred gently into 71-mL brown polyethylene bottles. The bottles were then processed in accordance with the method established by Kiene and Linn (2000*a*). These samples, amended with ^{35}S-$DMSP_d$ at trace level (final added concentration < 0.1 nmol L^{-1} $DMSP_d$), allowed the determination of five parameters: (1) the microbial $DMSP_d$ loss rate constant (k), calculated as the slope of the ln-transformed activity of unconsumed ^{35}S-$DMSP_d$ during the 3-h time course; (2) the microbial $DMSP_d$ consumption rate, calculated by multiplying the loss rate constant by the in situ concentration of $DMSP_d$; (3) the $DMSP_d$ turnover time (1/k); (4) the bacterial DMS yield, expressed as a percentage, which was taken as the fraction of ^{35}S-$DMSP_d$ consumed by bacteria that was recovered as ^{35}S-DMS at

the end of the 3-h incubations; and (5) the bacterial DMSP-S assimilation efficiency, also expressed as a percentage, calculated as the proportion of ^{35}S-DMSP$_d$ consumed by bacteria and recovered into trichloroacetic acid–insoluble macromolecules. Based on the recent discovery that some marine phytoplankton can accumulate sulfur from DMSP$_d$ (Vila-Costa et al. 2006), the DMSP$_d$ loss rate constant, consumption rates, and turnover rates as measured with this protocol are considered to be microbial (bacterioplankton and phytoplankton), while the ^{35}S-DMS yields are assumed to be mainly due to bacterial processing of DMSP, although algal DMSP-lyase activity cannot be excluded.

Statistical tests—Normality of the data was assessed using the Shapiro–Wilk test, from which nonparametric statistics were preferred over parametric analysis. Spearman correlation coefficients were used to quantify the strength of the association between the different variables. All statistical analyses were performed using the statistical softwares Sigma Plot 11 and Mat Lab 7.6.0.

Results

Oceanographic setting—The physical and biochemical characteristics of the water column during the study were typical of spring and summer conditions in the NE subarctic Pacific. Temperature at 10 m depth was relatively uniform at ca. 11°C at Stas. P1 to P8, and decreased toward the oceanic stations, to reach 7.1°C at P26 (Fig. 2A). Salinity at 10 m depth was ca. 31.5 at P1 and P4, remained relatively uniform at 32.4 from P8 to P16, and then gradually increased to reach 32.6 at P26 (Fig. 2A).

Nutrient salts $NO_3^- + NO_2^-$, H_4SiO_4, and PO_4^{3-} concentrations were high at P1 (8.9, 22.7, and 1.0 μmol L^{-1}), reached minima at P4 (0.1, 2.1, and 0.27 μmol L^{-1}), increased again at P8 (5.8, 9.4, and 0.91 μmol L^{-1}), and continued to increase up to P26 (Fig. 2B). TDFe concentrations were high at P1 and P4, with a mean value of 3.41 nmol L^{-1}, decreased sharply to 1.78 nmol L^{-1} at P8, remained close to 1.0 nmol L^{-1} between P14 and P18, and exhibited values below 0.79 nmol L^{-1} for the rest of the transect (Fig. 2C). There is no TDFe value at P12 due to contamination during the sampling. TDFe concentrations decreased with increasing water density (sigma-t) along the transect ($\rho = -0.89$; $p < 0.001$), indicating a gradual loss of Fe as the Fe-rich coastal waters mix with the Fe-poor denser HNLC waters. The correlation between TDFe and sigma-t was also significant ($\rho = -0.79$; $p < 0.001$) when only the offshore stations were considered (P8 to P26), showing the fertilization of the Alaska Current by the North Pacific Current.

Chl a *concentrations and phytoplankton community composition*—Chl *a* concentration was maximum (8.4 μg L^{-1}) at P1, decreased abruptly to reach 0.3 μg L^{-1} at P8, and remained below 0.5 μg L^{-1} for the rest of the transect (Fig. 3A). The results of the CHEMTAX analysis showed that prymnesiophytes were consistently the dominant phytoplankton group at the offshore stations (P12 to P26), representing on average 0.17 μg Chl *a* L^{-1} (Fig. 3B), and 44% of total pigment (data not shown). In contrast, diatoms dominated at P4 (0.33 μg Chl *a* L^{-1}). Cryptophytes were on average the second most important phytoplankton group along the transect, with concentrations varying between 0.05 and 0.20 μg Chl *a* L^{-1}. The relative contribution of cyanobacteria increased toward the shore with values of 0.01 and 0.11 μg Chl *a* L^{-1} at P26 and P4, respectively. The contribution of the other phytoplankton groups were variable and showed no obvious trend along the transect.

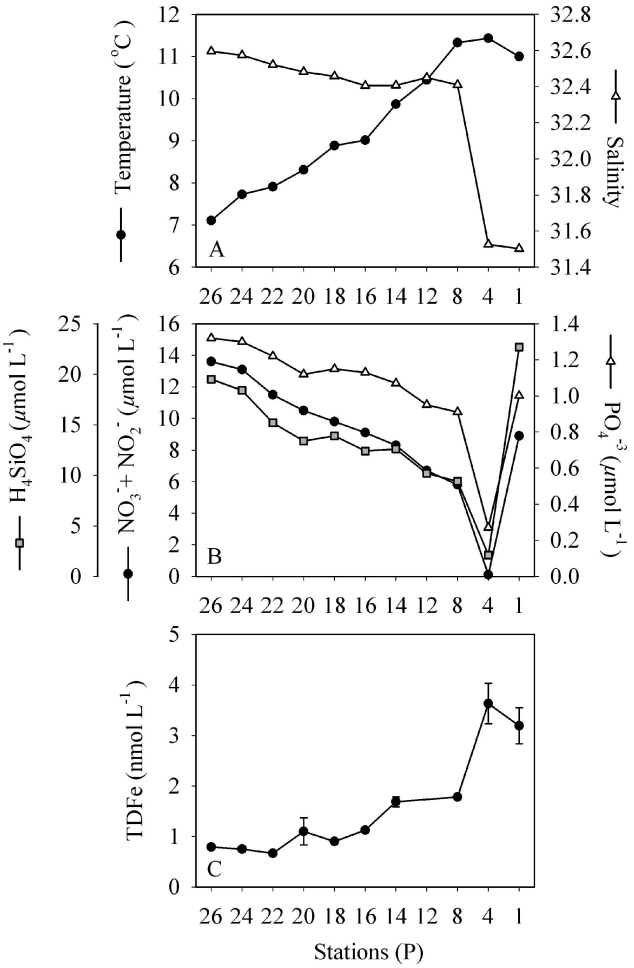

Fig. 2. Spatial variations in (A) temperature and salinity; (B) macronutrient concentrations; and (C) TDFe concentrations along the May–June 2007 Line P cruise transect in the NE Subarctic Pacific Ocean. There is no TDFe measurement at P12 because of contamination.

Heterotrophic bacterial abundance and community composition—Bacterial abundance (estimated with DAPI) was relatively high at P1 (2.1×10^9 cells L^{-1}) and P4 (3.9×10^9 cells L^{-1}), decreased abruptly to 1.05×10^9 cells L^{-1} at P8, and remained below 0.82×10^9 cells L^{-1} for the rest of the transect (Fig. 4A). The three clades targeted during our study exhibited different distributions along the transect. *Roseobacter* (Ros536 probe) concentrations were high at P1 (0.32×10^9 cells L^{-1}) and P4 (0.43×10^9 cells L^{-1}) and

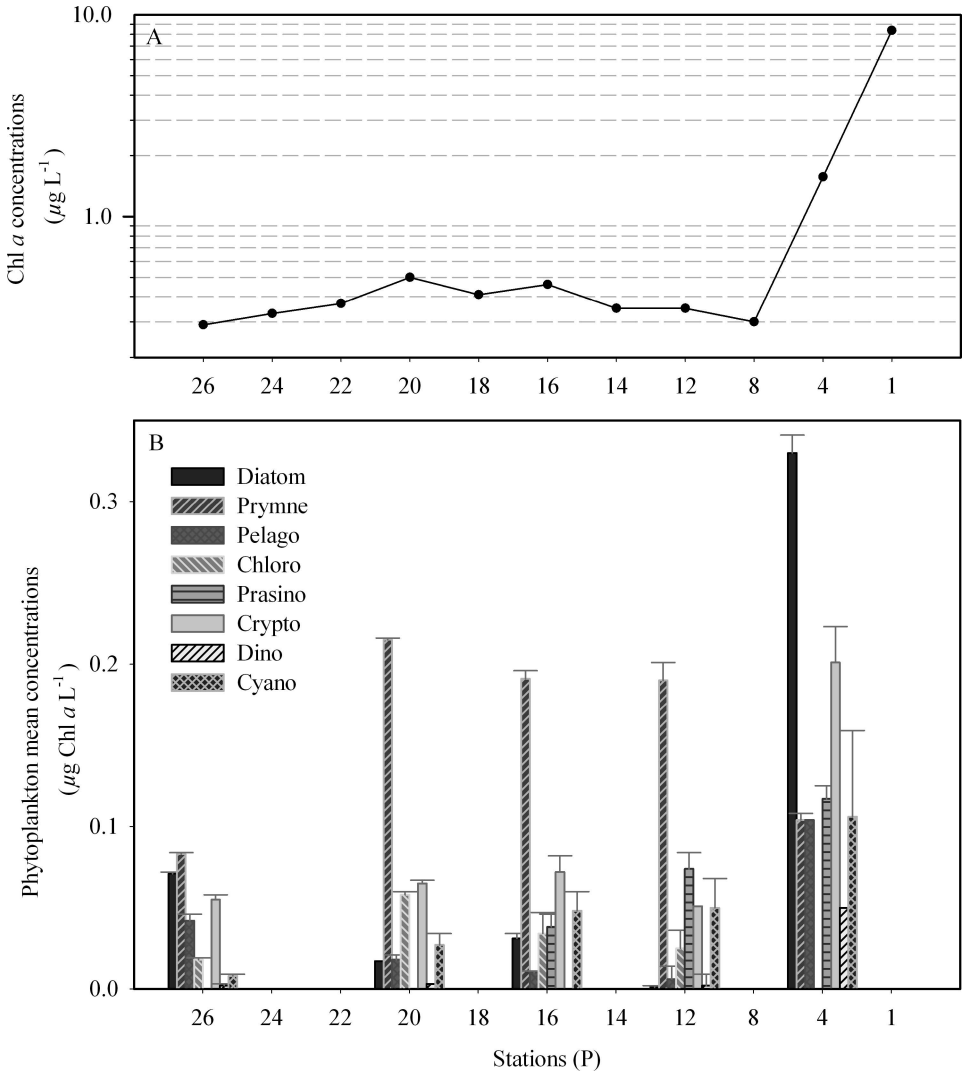

Fig. 3. Spatial variations in (A) Chl *a* concentrations and (B) the abundance of each phytoplankton group in Chl *a* units along the May–June 2007 Line P transect in the NE Subarctic Pacific Ocean. The error bars indicate the standard deviation calculated from CHEMTAX duplicates.

decreased to a mean concentration of 0.08×10^9 cells L^{-1} at the offshore stations (Fig. 4B). The abundance of *Gammaproteobacteria* (Gam42a probe) was more variable along the transect, with peak values at P4 (0.21×10^9 cells L^{-1}) and P16 (0.27×10^9 cells L^{-1}), and lowest values ($< 0.03 \times 10^9$ cells L^{-1}) between P20 and P26 (Fig. 4C). *Betaproteobacteria* (Bet42a probe) were more abundant at P4 (0.07×10^9 cells L^{-1}) and P8 (0.06×10^9 cells L^{-1}), and their abundance decreased more or less regularly toward the offshore stations to reach a minimum value of 0.007×10^9 cells L^{-1} at P26 (Fig. 4D). The abundances of total bacteria and of the three bacterial clades were positively correlated with TDFe along the transect (Table 2). At the offshore stations (P8 to P26), only the *Betaproteobacteria* exhibited a significant (positive) correlation with TDFe (Table 2).

Concentrations and microbial metabolism of dimethylated sulfur compounds—Concentrations of $DMSP_p$ exhibited a progressive inshore–offshore decline with maximum and minimum concentrations of 102.1 and 17.8 nmol L^{-1} measured at P1 and P26, respectively (Fig. 5A). $DMSP_p$ concentrations were positively correlated with TDFe along the transect and at the offshore stations (Table 2). $DMSP_p$: Chl *a* ratios showed a different pattern, with values below 39 nmol μg^{-1} at the inshore stations (P1 and P4), a peak value of 171 nmol μg^{-1} at P8, followed by a gradual decrease to 52 nmol μg^{-1} toward the offshore stations (Fig. 5A). Variations in the $DMSP_p$: Chl *a* ratio were positively correlated with TDFe only at the offshore stations (Table 2). $DMSP_d$ concentrations ranged between 1.3 and 3.6 nmol L^{-1} with no consistent pattern related either to the $DMSP_p$ pool or to the different water masses sampled (Fig. 5B). DMS concentrations exhibited considerable variations, with peak values of 4.4 and 3.6 nmol L^{-1} at P8 and P22, respectively, and a minimum of 1.1 nmol L^{-1} at P14 (Fig. 5C). DMS concentrations normalized to Chl *a*

(DMS : Chl *a* ratio; Table 3) were low at the inshore stations (0.3 and 1.6 nmol μg^{-1} at P1 and P4, respectively) and increased to ca. 6.2 ± 3.8 nmol μg^{-1} at the other stations (P8–P26).

The $DMSP_d$ loss rate constant (k), a measure of the affinity of the microbial assemblage for $DMSP_d$, varied between 2.1 d^{-1} (P26) and 22.1 d^{-1} (P4) along the transect, with the highest and lowest values measured at the inshore and offshore stations, respectively (Fig. 5D; Table 3). Variations in k were positively correlated with *Roseobacter* and *Gammaproteobacteria* (Table 2). Microbial $DMSP_d$ consumption rates (k × $DMSP_d$ concentrations) were high near the coast with values of 26.3 nmol L^{-1} d^{-1} at P1 and 57.9 nmol L^{-1} d^{-1} at P4, and lower offshore with an average of 8.6 nmol L^{-1} d^{-1} at Stas. P8 to P26 (Table 3). The microbial turnover time of the $DMSP_d$ pool (1/k) ranged from a rapid mean value of 2.5 h at inshore stations to a much longer mean value of 7.7 h at offshore stations (Table 3). The bacterial DMS yields ranged from 3% to 13% along the transect, with values higher in the HNLC waters (8% ± 2%) and lower in the coastal waters (5.6% and 3.1%) (Fig. 5E; Table 3). Variations in DMS yields showed no significant correlation with the abundance of bacteria, nor with any of the specific clades tested (Table 2). The bacterial DMSP-S assimilation efficiency, which represents the proportion of ^{35}S-DMSP assimilated into macromolecules, was 23% and 29% at the two Fe-rich inshore stations and ca. 12% ± 3% at the offshore stations (Fig. 5F; Table 3). Variations in bacterial DMSP-S assimilation efficiency were positively correlated with *Roseobacter* abundance (Table 2). Note that the DMSP-S assimilation efficiencies are not shown for Stas. P12 and P18 because of atypical variability between the two replicates rendering the value unreliable.

Discussion

The physical and chemical conditions encountered during our study were typical of the NE subarctic Pacific during late spring and early summer (Crawford et al. 2007; Peña and Varela 2007). Lower salinities at the inshore stations reflect freshwater supply from land. As expected, coastal waters were Fe-rich and exhibited moderate (1.6 μg L^{-1}) to high (8.4 μg L^{-1}) Chl *a* concentrations dominated by diatoms (Fig. 3). Macronutrient concentrations were high at P1 but were almost exhausted at P4, a condition previously reported for this station at this time of the year (Sherry et al. 2002) and which reflects a declining phytoplankton bloom (Boyd and Harrison 1999). Salinity increased steeply from P4 to P8, to reach values more typical of the North Pacific Current. Even though the TDFe concentration at P8 (1.78 nmol L^{-1}) was relatively high, macronutrient concentrations were high and phytoplankton biomass was low, consistent with the HNLC conditions expected at this station of the Line P transect (Harrison et al. 1999). The negative correlation calculated between TDFe and sigma-t at 10 m (Table 2) suggests that the distribution of TDFe was largely determined by the lateral and vertical mixing between the Fe-rich coastal waters, the North Pacific Current, and the Alaska Current.

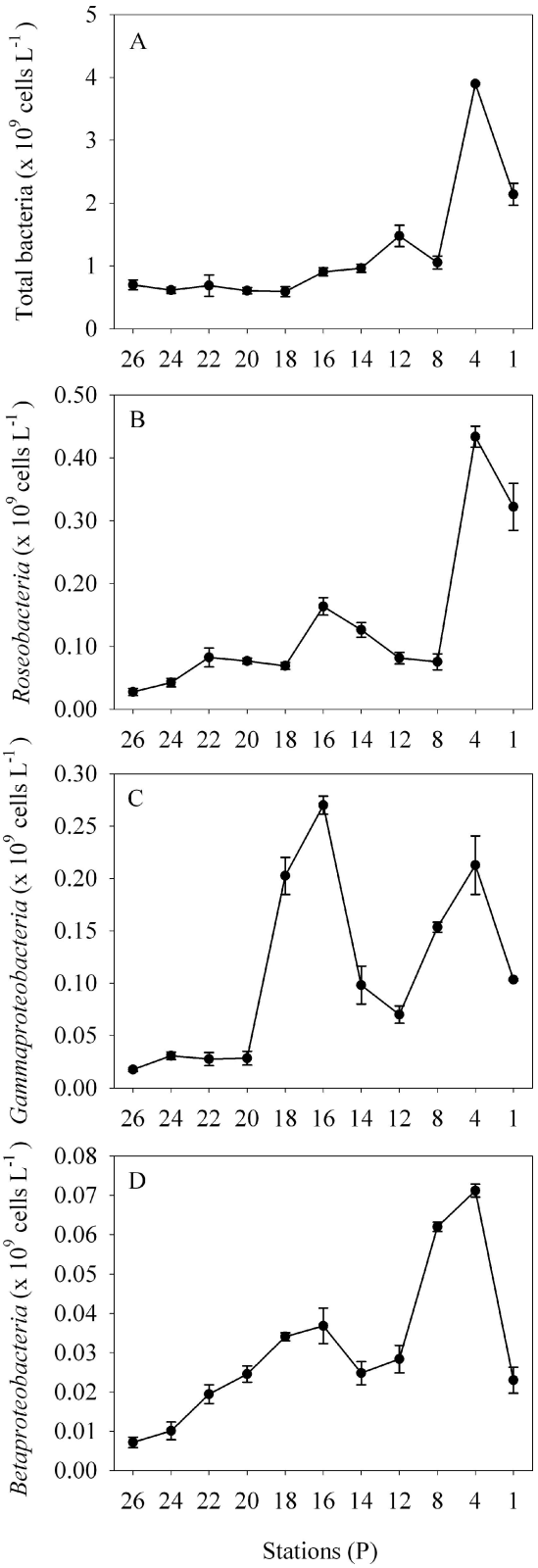

Fig. 4. Spatial variations in the abundance of (A) total bacteria; (B) *Roseobacter* (Ros536); (C) *Gammaproteobacteria* (γ, Gam42a); and (D) *Betaproteobacteria* (β, Bet42a) using the CARD-FISH technique along the May–June 2007 Line P cruise transect in the NE subarctic Pacific Ocean. Note the different scales of the *y*-axes. The error bars indicate the standard deviation calculated from counts of duplicate microscopic slides.

Table 2. Spearman's rank correlation coefficients (ρ) conducted on variables at all stations along the transect (P1–P26) and at stations within the HNLC waters (P8–P26). (*** $p < 0.001$; ** $p < 0.01$; * $p < 0.05$).

Variables		Spearman's correlation coefficients (ρ)	
		P1–P26	P8–P26
Sigma-t	TDFe	−0.89***	−0.75***
TDFe	$DMSP_p$	0.88***	0.79*
	$DMSP_p$: Chl *a*	−0.09	0.76*
	Total bacterial abundance	0.73*	0.48
	Roseobacter abundance	0.68*	0.38
	Gammaproteobacteria abundance	0.67*	0.62
	Betaproteobacteria abundance	0.72*	0.81**
Microbial $DMSP_d$ loss rate constant (k)	Total bacterial abundance	0.46	0.02
	Roseobacter abundance	0.65*	0.37
	Gammaproteobacteria abundance	0.63*	0.52
	Betaproteobacteria abundance	0.38	0.37
Bacterial DMS yield	$DMSP_p$: Chl *a*	0.82***	0.68*
	Total bacterial abundance	−0.23	0.42
	Roseobacter abundance	−0.49	−0.07
	Gammaproteobacteria abundance	−0.42	−0.22
	Betaproteobacteria abundance	−0.04	0.20
Bacterial DMSP-S assimilation efficiency	Total bacterial abundance	0.45	0.18
	Roseobacter abundance	0.77*	0.50

Based on the physical, chemical, and biological properties, stations along the transect were subdivided into two categories exhibiting distinct TDFe levels and supply modes: the Fe-rich coastal waters (P1 and P4), where TDFe concentrations were high and probably primarily delivered through river input, and the HNLC waters (P8 to P26), where TDFe concentrations were generally low and primarily delivered through vertical and lateral mixing of waters from the Alaska and the North Pacific Currents.

DMSP and phytoplankton assemblage—$DMSP_p$ concentrations decreased by a factor of 6 from inshore to offshore, following the general decline in Chl *a* (Figs. 3A, 5A). $DMSP_p$ and Chl *a* were, however, not significantly correlated across the transect due to the large inshore–offshore variations in $DMSP_p$: Chl *a* ratios (see below). Few $DMSP_p$ measurements have been reported so far from the open waters of the NE Pacific, and none have been reported in coastal waters. The only data available are from the July 2002 SERIES experiment, where Levasseur et al. (2006) measured $DMSP_p$ concentrations between 5 and 75 nmol L^{-1} around P26 outside the Fe-enriched patch. In the present study, $DMSP_p$ levels between 17 and 51 nmol L^{-1} in the HNLC waters compare well with the SERIES values.

In spite of the large variations in the size of the $DMSP_p$ pool, concentrations of $DMSP_d$ remained low and relatively uniform along the transect, reflecting the labile nature and rapid bacterial turnover rate of this compound (Fig. 5B; Table 3). The $DMSP_d$ concentrations presented here are within the range previously reported by Kiene and Slezak (2006) in contrasting oceanic environments using the SVDF technique (from 0.4 to 2.8 nmol L^{-1}). Our results provide further support to the recent suggestion that low $DMSP_d$ concentrations (< 3 nmol L^{-1}) are typical of marine systems (Kiene and Slezak 2006), irrespective of the size of the $DMSP_p$ reservoir. They also extend this conclusion to HNLC waters.

The $DMSP_p$: Chl *a* ratios exhibited a similar inshore–offshore decrease as $DMSP_p$, but only in the HNLC portion of the transect (Fig. 5A; Table 2). The very low $DMSP_p$: Chl *a* ratios measured at the inshore biomass-rich stations reflect the dominance of DMSP-poor diatoms previously described in these waters (Boyd et al. 1996; Boyd and Harrison 1999). A similarly low ratio has been reported in the NE Atlantic during the spring diatom bloom (33 ± 18 nmol μg^{-1}; Andreae et al. 2003). In contrast, the high ratios in the HNLC waters reflect the dominance of prymnesiophytes (Fig. 3B). The phytoplankton assemblage in the HNLC waters of the NE subarctic Pacific is generally dominated by the prymnesiophytes *Emiliania huxleyi* and *Phaeocystis* spp. (Boyd and Harrison 1999; Levasseur et al. 2006), two strong DMSP producers (Keller et al. 1989). The dominance of these small algal cells is attributed to their capacity to compete under low-Fe conditions because of their high surface-to-volume ratios and their ability to implement low Fe-demand metabolic pathways (Martin et al. 1989; Sunda et al. 1991; Sunda and Huntsman 1997). Low Fe availability may thus favor the development of strong DMSP producers (Malin and Kirst 1997), hence explaining the higher ratios of $DMSP_p$: Chl *a* observed in the HNLC waters (Fig. 5A).

DMSP microbial uptake and metabolism—The microbial affinity for $DMSP_d$ (k) varied in concert with the distribution of *Roseobacter*, a member of *Alphaproteobacteria*, and with *Gammaproteobacteria* (Table 2), both important contributors to DMSP metabolism (Malmstrom et al. 2004*a*,*b*; Vila et al. 2004; Vila-Costa et al. 2007). The mean microbial $DMSP_d$ consumption rates measured at the

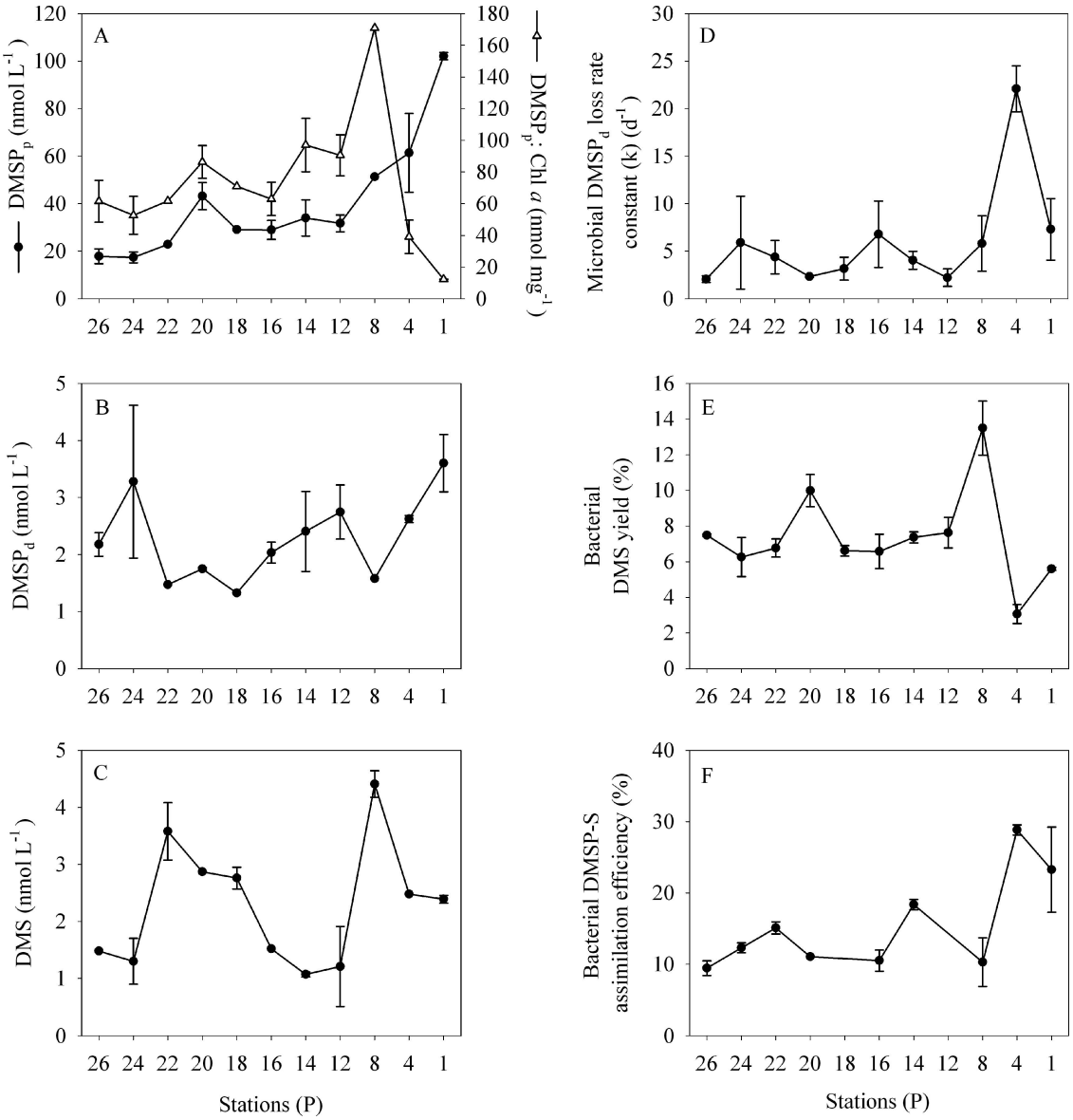

Fig. 5. Spatial variations in (A) $DMSP_p$ concentrations and $DMSP_p$: Chl a ratio, (B) $DMSP_d$ concentrations, (C) DMS concentrations, (D) microbial $DMSP_d$ loss rate constant (k), (E) bacterial DMS yields, and (F) bacterial DMSP-S assimilation efficiencies along the May–June 2007 Line P cruise transect in the NE subarctic Pacific Ocean. The error bars indicate the standard deviation calculated from duplicates.

inshore (42 nmol L^{-1} d^{-1}) and offshore (8.6 nmol L^{-1} d^{-1}) stations are comparable with those reported for the biomass-rich coastal waters of the Gulf of Mexico (39 nmol L^{-1} d^{-1}) and for the oligotrophic waters of the Sargasso Sea (3.8 nmol L^{-1} d^{-1}) (Kiene et al. 2000). Owing to the relative stability of the $DMSP_d$ pool size, the changes in microbial $DMSP_d$ consumption rates resulted in similar changes in $DMSP_d$ turnover times (Table 3). The mean $DMSP_d$ turnover times measured during this study for the inshore and offshore stations were remarkably similar to values reported for environments with comparable biological productivities. For example, Kiene and Linn (2000*b*) measured $DMSP_d$ turnover times of 3 h in shelf waters and of 10 h in oceanic waters, while Malmstrom et al. (2004*b*) and Zubkov et al. (2002) showed $DMSP_d$ turnover times of 11–28 h and 9.6 h for the Sargasso Sea and the North Sea, respectively. These results suggest that the microbial consumption of DMSP varies primarily with the overall productivity of the ecosystem, probably reflecting the ubiquity of the bacterial DMSP consumers in natural assemblages.

The inshore and offshore bacterial assemblages exhibited distinct DMSP metabolisms (Fig. 5E,F). The DMS yields were consistently higher offshore than inshore, suggesting that the DMSP-rich assemblages thriving in the HNLC portion of the transect were more efficient in producing DMS than the coastal communities. In Fe-poor waters, where the production of labile dissolved carbon by

Table 3. Means and ranges measured at Fe-rich inshore stations (P1 and P4), and means and standard deviations (SD) measured at Fe-poor offshore stations (P8 to P26) for different variables along Line P.

Variables	Fe-rich inshore stations		Fe-poor offshore stations	
	mean (n = 2)	range	mean (n = 9)	SD
$DMSP_p$ (nmol L^{-1})	82	61–102	31	11
$DMSP_d$ (nmol L^{-1})	3.1	2.6–3.6	2.1	0.6
DMS (nmol L^{-1})	2.4	2.4–2.5	2.2	1.2
$DMSP_p$: Chl *a* ratio (nmol μg^{-1})	26	12–39	84	36
DMS : Chl *a* ratio (nmol μg^{-1})	0.9	0.3–1.6	6.2	3.8
Microbial $DMSP_d$ loss rate constant (k) (d^{-1})	14.7	7.3–22.1	4.1	1.8
Microbial $DMSP_d$ consumption rate (nmol L^{-1} d^{-1})	42	26–58	8.6	5.1
Microbial $DMSP_d$ turnover time (h)	2.5	1.3–3.7	7.7	3.0
Bacterial DMSP-S assimilation efficiency (%)	26	23–28	12	3
Bacterial DMS yield (%)	4	3.1–5.6	8	2

phytoplankton is thought to be weak (Kirchman 1990), bacteria are generally limited by the availability of organic carbon. More recently, Hale et al. (2006) demonstrated that the availability of organic carbon was indeed limiting bacterial productivity around P26 during SERIES. In these conditions, bacteria may increase the proportion of DMSP used as a carbon source through the cleavage pathway, which would lead to higher bacterial DMS yields as reported here.

The positive correlation found during our study between DMS yields and $DMSP_p$: Chl *a* ratios (Table 2) probably also reflects the prevalence of strong DMSP producers in Fe-poor waters. This result is consistent with the observation by Vila-Costa et al. (2008) of a positive relationship between DMS production and the $DMSP_p$: Chl *a* ratios during a seasonal cycle in the coastal NW Mediterranean Sea. As discussed below, this relationship may not be strictly bacterial but could also result from an increased contribution of algal DMSP-lyase activity to the total DMS production.

The inshore and offshore stations were also characterized by different DMSP-S assimilation efficiencies (Fig. 5F). The consistently low DMSP-S assimilation efficiencies measured in the Fe-poor Alaska Current indicate a low bacterial sulfur demand, probably resulting from a shortage in labile organic carbon as discussed above. At the inshore stations, the higher bacterial abundance seems to have led to a slightly greater fraction of DMSP-S being assimilated into bacterial proteins and to a lower fraction being lost as DMS. A similar inshore vs. offshore pattern has been reported by Kiene and Linn (2000*b*), who showed high bacterial DMSP-S assimilation into macromolecules in coastal waters (mean of 44% ± 21%), while lower DMSP-S assimilation efficiencies were observed in oceanic waters (mean of 12% ± 7%). The tendency of the DMSP-S assimilation efficiency to increase from offshore to inshore as *Roseobacter* abundances rose (Table 2) probably reflects an increase in growth and S-demand of this clade following a relaxation of Fe stress and enhanced availability of labile organic carbon. This interpretation is consistent with the observation by Lizotte et al. (2009) of an increase in bacterial DMSP-S assimilation efficiency following Fe-induced increases in bacterial abundance and productivity during the Subarctic Pacific Iron Experiment for Ecosystem Dynamics Study II (SEEDS II) in the northwest (NW) subarctic Pacific.

In spite of the inshore–offshore differences in DMS yields mentioned above, DMSP cleavage into DMS remained a minor metabolic pathway during our study. The range of DMS yields measured along the transect (3–14%; Fig. 5E) was comparable to the range of 2% to 21% reported earlier in a study of coastal, shelf, and oceanic waters (Kiene and Linn 2000*b*), as well as with the range of values (7–13%) reported for an HNLC region of the NW subarctic Pacific (Lizotte et al. 2009). Our DMS yield values agree with mounting evidence suggesting that most of the $DMSP_d$ consumed by the microbial community (> 86% in our study) is processed through the demethylation pathway without the formation of DMS.

DMS distribution and turnover time—We found no significant relationships between DMS concentrations and the different bacterial rate measurements conducted during our study. This apparent lack of direct relationship is expected given the numerous and diverse abiotic and biotic factors controlling the concentrations of DMS in surface waters (*see* review by Simó 2001). In that respect, the comparison between our bacterial rate measurements and the in situ DMS concentrations suggests that a large part of the DMS production could have been mediated by nonbacterial activity at the offshore stations, where we calculated a mean microbial DMS production rate of 0.7 nmol L^{-1} d^{-1} ($DMSP_d$ consumption rate of 8.6 nmol L^{-1} d^{-1} multiplied by DMS yield of 0.08). Assuming steady-state conditions, this production rate seems insufficient to sustain a mean DMS concentration of 2.2 nmol L^{-1}, implying a lengthy turnover time of 3 d. On the other hand, at the inshore stations, our calculated mean microbial DMS production rate of 1.6 nmol L^{-1} d^{-1} could probably sustain the measured 2.4 nmol L^{-1} of DMS with a turnover time of only 1 d. The results suggest the presence of nonbacterial DMS sources at the offshore stations, most probable being direct or indirect (through microzooplankton grazing) release from the dominant prymnesiophytes with known DMSP-lyase activity.

Sensitivity of the HNLC plankton assemblages to TDFe—A closer look at the offshore portion of the transect

provides further information on how HNLC plankton assemblages respond to Fe fertilization via mixing. Between P8 and P26, TDFe concentrations increased as the Alaska Current waters mixed with the North Pacific Current waters (Fig. 1). As this mixing proceeded, the resulting increase in TDFe was accompanied by an increase in $DMSP_p$ and $DMSP_p$: Chl *a* ratios (Table 2). Although the Fe status of the phytoplankton was not determined during our study, the results suggest that the addition of Fe by mixing increased the abundance or the DMSP quotas of the microalgae thriving at the low Fe offshore stations. CHEMTAX analysis is available only for four stations in this portion of the transect (Fig. 3B), which prevents the exploration of statistical relationships between variations in $DMSP_p$ and the abundance of specific taxa. It is, however, noteworthy that Stas. P12, P16, and P20, which show a high abundance of prymnesiophytes, also have high levels of $DMSP_p$ as compared to P26, which exhibits low levels of prymnesiophytes and $DMSP_p$ (Figs. 3, 5A). This suggests that the increase in $DMSP_p$: Chl *a* ratio in the HNLC waters could have resulted, at least partially, from an increase in the abundance of the DMSP-rich species. This interpretation of our results is consistent with the reported rapid increases in $DMSP_p$ due to a stimulation of the prymnesiophytes over the first days of most OIFs (Turner et al. 2004; Levasseur et al. 2006).

In the HNLC portion of the transect, *Betaproteobacteria* abundance increased with TDFe. However, none of the DMSP-related bacterial rates exhibited a significant correlation with TDFe (Table 2). The small contribution of the *Betaproteobacteria* to the total bacterial abundance ($< 5\%$) may explain their apparent lack of impact on DMSP uptake and metabolism. During SEEDS II, the sole OIF reporting similar measurements, the Fe fertilization resulted in a rapid increase in bacterial abundance and DMSP-S assimilation efficiency and in a decrease in DMS yield (Lizotte et al. 2009). The difference between the two studies suggests that bacteria may respond differently depending of the mode of Fe supply (direct fertilization vs. mixing).

Conclusions

The Line P transect in the NE subarctic Pacific offered an opportunity to characterize the distribution and bacterial metabolism of DMSP in two distinct and contrasting environments: the nutrient-rich diatom-dominated inshore waters and the Fe-poor prymnesiophyte-dominated offshore waters. In addition, the gradient in TDFe found in the HNLC portion of the transect prompted us to explore potential responses of the thriving plankton assemblages to this natural Fe input.

We highlighted important differences in $DMSP_p$: Chl *a* ratios and bacterial DMSP metabolism between the inshore and offshore waters. Offshore HNLC stations had higher $DMSP_p$: Chl *a* ratios than the inshore stations, reflecting the dominance of DMSP-rich prymnesiophytes. The stations also exhibited higher DMS yields and lower DMSP-S assimilation efficiencies compared to inshore stations. This suggests a greater proportional use of DMSP as a carbon source rather than a sulfur source under HNLC conditions, probably resulting from the carbon-limited status of the bacteria. In contrast, bacteria used DMSP mostly as a sulfur source in the biomass-rich coastal waters where labile dissolved organic carbon is probably plentiful. In spite of the inshore–offshore differences in DMSP metabolism, the importance of DMSP as a substrate for bacteria was reflected in the close relationship between the $DMSP_d$ loss rate constant (k) and the abundance of *Roseobacter* and *Gammaproteobacteria* all across the transect.

As the Fe-poor Alaska Current waters mixed with the North Pacific Current waters, we measured a gradual increase in TDFe concentrations, while other biochemical parameters (macronutrients, Chl *a*, phytoplankton assemblages) still reflected HNLC conditions. This positive Fe gradient was accompanied by increases in DMSP concentrations and $DMSP_p$: Chl *a* ratios, suggesting a stimulation of the DMSP producers. The response of the bacteria to the TDFe gradient was more subtle, with only the poorly represented *Betaproteobacteria* showing a positive correlation with TDFe. Microbial DMSP uptake and bacterial DMSP metabolism were apparently not affected by the variations in TDFe.

The increase in $DMSP_p$ with the increase in TDFe concentrations measured during this study and most OIFs, including SERIES, suggest that the stimulation of DMSP dynamics will take place whatever the Fe supply mode: atmospheric dust deposition or vertical and lateral mixing. However, the results from the few studies available suggest a less consistent response of the bacterial assemblages and DMSP metabolism.

Acknowledgments

We thank the officers, crew, and fellow scientists onboard the CCGS *John P. Tully* for assistance during the cruise; Janet Barwell-Clarke and Wendy Richardson, who participated in chlorophyll *a* and macronutrient measurements during the cruise; Melanie Quenneville, who generously let us use her radioactivity laboratory at the Institute of Ocean Sciences (Sidney, Canada); Nes Sutherland for the iron measurements; and two anonymous reviewers for their constructive comments on an earlier draft of this manuscript. This project was supported by grants to M.L. from the Natural Sciences and Engineering Research Council (NSERC). S.-J.R. received scholarships from Québec-Océan and the Biology department of Université Laval. The Line P program is sponsored by Fisheries and Oceans Canada.

References

Andreae, M. O. 1990. Ocean-atmosphere interactions in the global biogeochemical sulfur cycle. Mar. Chem. **30:** 1–29, doi:10.1016/0304-4203(90)90059-L

———, T. W. Andreae, D. Meyerdierks, and C. Thiel. 2003. Marine sulfur cycling and the atmospheric aerosol over the springtime North Atlantic. Chemosphere **52:** 1321–1343, doi:10.1016/S0045-6535(03)00366-7

Barwell-Clarke, J., and F. Whitney. 1996. Institute of ocean sciences nutrient methods and analysis. Can. Tech. Rep. Hydrogr. Ocean Sci. **182:** vi + 43.

Bopp, L., O. Aumont, S. Belviso, and S. Blain. 2008. Modelling the effect of iron fertilization on dimethylsulphide emissions in the Southern Ocean. Deep-Sea Res. II **55:** 901–912, doi:10.1016/j.dsr2.2007.12.002

Boyd, P. W., and P. J. Harrison. 1999. Phytoplankton dynamics in the NE subarctic Pacific. Deep-Sea Res. II **46:** 2405–2432, doi:10.1016/S0967-0645(99)00069-7

———, D. L. Muggli, D. E. Varela, R. H. Goldblatt, R. Chretien, K. J. Orians, and P. J. Harrison. 1996. In vitro iron enrichment experiments in the NE Subarctic Pacific. Mar. Ecol. Prog. Ser. **136:** 179–193, doi:10.3354/meps136179

———, and others. 2004. The decline and fate of an iron-induced subarctic phytoplankton bloom. Nature **428:** 549–553, doi:10.1038/nature02437

———, and others. 2007. Mesoscale iron enrichment experiments 1993–2005: Synthesis and future directions. Science **31:** 612–617, doi:10.1126/science.1131669

Charlson, R. J., J. E. Lovelock, M. O. Andreae, and S. G. Warren. 1987. Oceanic phytoplankton, atmospheric sulphur, cloud albedo and climate. Nature **326:** 655–661, doi:10.1038/326655a0

Crawford, W. R., P. J. Brickley, and A. C. Thomas. 2007. Mesoscale eddies dominate surface phytoplankton in northern Gulf of Alaska. Prog. Oceanogr. **75:** 287–303, doi:10.1016/j.pocean.2007.08.016

de Baar, H. J. W., J. T. M. de Jong, R. F. Nolting, K. R. Timmermans, M. A. van Leeuwe, U. Bathmann, R. van der Loeff, and J. Sildam. 1999. Low dissolved Fe and the absence of diatom blooms in remote Pacific waters of the Southern Ocean. Mar. Chem. **66:** 1–34, doi:10.1016/S0304-4203(99)00022-5

———, and others. 2005. Synthesis of iron fertilization experiments: From the Iron Age to the Age of Enlightenment. J. Geophys. Res. **110:** C09S16, doi:10.1029/2004JC002601

Freeland, H. 2007. A short history of Ocean Station Papa and Line P. Prog. Oceanogr. **75:** 120–125, doi:10.1016/j.pocean.2007.08.005

Hale, M. S., R. B. Rivkin, P. Matthews, N. R. S. Agawin, and W. K. W. Li. 2006. Microbial response to a mesoscale iron enrichment in the NE subarctic Pacific: Heterotrophic bacterial processes. Deep-Sea Res. II **53:** 2231–2247, doi:10.1016/j.dsr2.2006.05.039

Han, Y., X. Fang, T. Zhao, and S. Kang. 2008. Long range trans-Pacific transport and deposition of Asian dust aerosols. J. Environ. Sci. **20:** 424–428, doi:10.1016/S1001-0742(08)62074-4

Harrison, P. J., P. W. Boyd, D. E. Varela, S. Takeda, A. Shiomoto, and T. Odate. 1999. Comparison of factors controlling phytoplankton productivity in the NE and NW subarctic Pacific gyres. Prog. Oceanogr. **43:** 205–234, doi:10.1016/S0079-6611(99)00015-4

Hill, R. W., B. White, M. Cottrell, and J. W. H. Dacey. 1998. Virus-mediated release of demethylsulfoniopropionate from marine phytoplankton. Aquat. Microb. Ecol. **14:** 1–6, doi:10.3354/ame014001

Jickells, T. D., and others. 2005. Global iron connections between desert dust ocean biogeochemistry and climate. Science **308:** 67–71, doi:10.1126/science.1105959

Johnson, W. K., L. A. Miller, N. E. Sutherland, and C. S. Wong. 2005. Iron transport by mesoscale Haida eddies in the Gulf of Alaska. Deep-Sea Res. II **52:** 933–953, doi:10.1016/j.dsr2.2004.08.017

Keller, M. D., W. K. Bellows, and R. R. L. Guillard. 1989. Dimethyl sulfide production in marine phytoplankton, p. 167–182. *In* E. Saltzman and W. J. Cooper [eds.], Biogenic sulfur in the environment. American Chemical Society.

Kiene, R. P., and L. J. Linn. 2000*a*. The fate of dissolved dimethylsulfoniopropionate (DMSP) in seawater: Tracer studies using ^{35}S-DMSP. Geochim. Cosmochim. Acta **64:** 2797–2810, doi:10.1016/S0016-7037(00)00399-9

———, and ———. 2000*b*. Distribution and turnover of dissolved DMSP and its relationship with bacterial production and dimethylsulfide in the Gulf of Mexico. Limnol. Oceanogr. **45:** 849–861.

———, ———, and J. A. Bruton. 2000. New and important roles for DMSP in marine microbial communities. J. Sea Res. **43:** 209–224, doi:10.1016/S1385-1101(00)00023-X

———, and D. Slezak. 2006. Low dissolved DMSP concentrations in seawater revealed by small-volume gravity filtration and dialysis sampling. Limnol. Oceanogr.: Methods **4:** 80–95.

Kirchman, D. L. 1990. Limitation of bacterial growth by dissolved organic matter in the subarctic Pacific. Mar. Ecol. Prog. Ser. **62:** 47–54, doi:10.3354/meps062047

Lam, P. J., and J. K. B. Bishop. 2008. The continental margin is a key source of iron to the HNLC North Pacific Ocean. Geophys. Res. Lett. **35:** L07608, doi:10.1029/2008GL033294

Levasseur, M., and others. 2006. DMSP and DMS dynamics during a mesoscale iron fertilization experiment in the Northeast Pacific. Part I. Temporal and vertical distributions. Deep-Sea Res. II **53:** 2353–2369, doi:10.1016/j.dsr2.2006.05.023

Lizotte, M., M. Levasseur, I. Kudo, K. Suzuki, A. Tsuda, R. P. Kiene, and M. G. Scarratt. 2009. Iron-induced alterations of bacterial DMSP metabolism in the western subarctic Pacific during SEEDS-II. Deep-Sea Res. II **56:** 2889–2898, doi:10.1016/j.dsr2.2009.06.012

Mackey, M. D., D. J. Mackey, H. W. Higgins, and S. H. Wright. 1996. CHEMTAX—A program for estimating class abundances from chemical markers: Application to HPLC measurements of phytoplankton. Mar. Ecol. Prog. Ser. **144:** 265–283, doi:10.3354/meps144265

Malin, G., and G. O. Kirst. 1997. Algal production of dimethyl sulfide and its atmospheric role. J. Phycol. **33:** 889–896, doi:10.1111/j.0022-3646.1997.00889.x

———, W. H. Wilson, G. Bratbak, P. S. Liss, and N. H. Mann. 1998. Elevated production of dimethylsulfide resulting from viral infection of cultures of *Phaeocystis pouchetii*. Limnol. Oceanogr. **43:** 1389–1393.

Malmstrom, R. R., R. P. Kiene, M. T. Cottrel, and D. L. Kirchman. 2004*a*. Contribution of SAR11 bacteria to dissolved dimethylsulfoniopropionate and amino acid uptake in the North Atlantic Ocean. Appl. Environ. Microbiol. **70:** 4129–4135, doi:10.1128/AEM.70.7.4129-4135.2004

———, ———, and D. L. Kirchman. 2004*b*. Identification and enumeration of bacteria assimilating dimethylsulfoniopropionate (DMSP) in the North Atlantic and Gulf of Mexico. Limnol. Oceanogr. **49:** 597–606.

Martin, J. H., R. M. Gordon, S. Fitzwater, and W. W. Broenkow. 1989. VERTEX: Phytoplankton/iron studies in the Gulf of Alaska. Deep-Sea Res. **36:** 649–680.

Merzouk, A., and others. 2006. DMSP and DMS dynamics during a mesoscale iron fertilization experiment in the Northeast Pacific. Part II. Biological cycling. Deep-Sea Res. II **53:** 2370–2383, doi:10.1016/j.dsr2.2006.05.022

Moore, J. K., and O. Braucher. 2007. Observations of dissolved iron concentrations in the World Ocean: Implications and constraints for ocean biogeochemical models. Biogeosci. Discov. **4:** 1241–1277.

———, S. C. Doney, D. M. Glover, and I. Y. Fung. 2002. Iron cycling and nutrient-limitation patterns in surface waters of the World Ocean. Deep-Sea Res. II **49:** 463–507, doi:10.1016/S0967-0645(01)00109-6

Obata, H., H. Karatani, M. Matsui, and E. Nakayama. 1997. Fundamental studies for chemical speciation of iron in seawater with an improved analytical method. Mar. Chem. **56:** 97–106, doi:10.1016/S0304-4203(96)00082-5

———, ———, and E. Nakayama. 1993. Automated determination of iron in seawater by chelating resin concentration and chemiluminenscence detection. Anal. Chem. **65:** 1524–1528, doi:10.1021/ac00059a007

Peña, M. A., and D. E. Varela. 2007. Seasonal and interannual variability in phytoplankton and nutrient dynamics along Line P in the NE subarctic Pacific. Prog. Oceanogr. **75:** 200–222, doi:10.1016/j.pocean.2007.08.009

Pernthaler, A., J. Pernthaler, and R. Amann. 2002. Fluorescence in situ hybridization and catalyzed reporter deposition for the identification of marine bacteria. Appl. Environ. Microbiol. **68:** 3094–3101, doi:10.1128/AEM.68.6.3094-3101.2002

Porter, K. G., and Y. S. Feig. 1980. The use of DAPI for identifying and counting aquatic microflora. Limnol. Oceanogr. **25:** 943–948, doi:10.4319/lo.1980.25.5.0943

Scarratt, M. G., G. Cantin, M. Levasseur, and S. Michaud. 2000. Particle size-fractionated kinetics of DMS production: Where does DMSP cleavage occur at the microscale? J. Sea Res. **43:** 245–252, doi:10.1016/S1385-1101(00)00019-8

Sherry, N. D., B. Imanian, K. Sugimoto, P. W. Boyd, and P. J. Harrison. 2002. Seasonal and interannual trends in heterotrophic bacterial processes between 1995 and 1999 in the subarctic NE Pacific. Deep-Sea Res. II **45:** 5775–5791, doi:10.1016/S0967-0645(02)00214-X

Simó, R. 2001. Production of atmospheric sulfur by oceanic plankton: Biogeochemical, ecological and evolutionary links. Trends Ecol. Evol. **16:** 287–294, doi:10.1016/S0169-5347(01)02152-8

Strickland, J. D. H., and T. R. Parsons. 1972. A practical handbook of sea-water analysis. 2nd ed. Journal of Fisheries Research Board of Canada.

Sunda, W. G., and S. A. Hunstman. 1997. Iron uptake and growth limitation in oceanic and coastal phytoplankton. Mar. Chem. **50:** 189–206, doi:10.1016/0304-4203(95)00035-P

———, D. G. Swift, and S. A. Huntsman. 1991. Low iron requirement for growth in oceanic phytoplankton. Nature **351:** 55–57, doi:10.1038/351055a0

Suzuki, K., C. Minami, H. Liu, and T. Saino. 2002. Temporal and spatial patterns of chemotaxonomic algal pigments in the subarctic Pacific and the Bering Sea during early summer of 1999. Deep-Sea Res. II **49:** 5685–5704, doi:10.1016/S0967-0645(02)00218-7

Turner, S. M., M. J. Harvey, C. S. Law, P. D. Nightingale, and P. S. Liss. 2004. Iron-induced changes in oceanic sulfur biogeochemistry. Geophys. Res. Lett. **31:** L14307, doi:10.1029/2004GL020296

Vila, M., R. Simó, R. P. Kiene, J. Pinhassi, J. M. González, M. A. Moran, and C. Pedrós-Alió. 2004. Use of microautoradiography combined with fluorescence in situ hybridization to determine dimethylsulfoniopropionate incorporation by marine bacterioplankton taxa. Appl. Environ. Microbiol. **70:** 4648–4657, doi:10.1128/AEM.70.8.4648-4657.2004

Vila-Costa, M., R. P. Kiene, and R. Simó. 2008. Seasonal variability of the dynamics of dimethylated sulfur compounds in a coastal northwest Mediterranean site. Limnol. Oceanogr. **53:** 198–211.

———, J. Pinhassi, C. Alonso, J. Pernthaler, and R. Simó. 2007. An annual cycle of dimethylsulfoniopropinate—sulfur and leucine assimilating bacterioplankton in the coastal NW Mediterranean. Environ. Microbiol. **9:** 2451–2463, doi:10.1111/j.1462-2920.2007.01363.x

———, R. Simó, H. Harada, J. M. Gasol, D. Slezak, and R. P. Kiene. 2006. Dimethylsulfoniopropionate uptake by marine phytoplankton. Science **314:** 652–654, doi:10.1126/science.1131043

Young, R. W., and others. 1991. Atmospheric iron inputs and primary productivity: Phytoplankton responses in the North Pacific. Glob. Biogeochem. Cycles **5:** 119–134, doi:10.1029/91GB00927

Yuan, W., and J. Zhang. 2006. High correlations between Asian dust events and biological productivity in the western North Pacific. Geophys. Res. Lett. **33:** L07603, doi:10.1029/2005GL025174

Zapata, M., F. Rodriguez, and J. L. Garrido. 2000. Separation of chlorophylls and carotenoids from marine phytoplankton: A new HPLC method using a reversed phase C8 column and pyridine-containing mobile phases. Mar. Ecol. Prog. Ser. **195:** 29–45, doi:10.3354/meps195029

Zubkov, M. V., B. M. Fuchs, S. D. Archer, R. P. Kiene, R. Amann, and P. H. Burkill. 2002. Rapid turnover of dissolved DMS and DMSP by defined bacterioplankton communities in the stratified euphotic zone of the North Sea. Deep-Sea Res. II **49:** 3017–3038, doi:10.1016/S0967-0645(02)00069-3

Associate editor: Mikhail V. Zubkov

Received: 30 July 2009
Accepted: 15 March 2010
Amended: 16 March 2010